Bull. Nov. Comp. Center, Num. Model. in Atmosph., etc., 11 (2007), 65–77

On the influence of the horizontal viscosity parametrization on the thermohaline circulation in the ocean model*

A.V. Scherbakov, V.V. Malakhova

Abstract. The three-dimensional seasonally forced linear model of the World ocean climate with a real bottom and 24 levels in the vertical coordinate has been developed. The computational domain includes the Arctic ocean. The numerical method is based on using the implicit schemes. The equations of heat and salt transport on a horizontal coordinates are approximated by the nine-dot difference scheme, obtained with the Richardson extrapolation. The second up-wind scheme is used in the vertical coordinate. The main objectives of the model are reconstructions of the ocean large-scale thermohaline circulation. The model circulation is forced by prescribing the wind stress and surface values of temperature and salinity. A global distribution of temperature and salinity fields is in agreement with observations. This paper reports the results from the coarse-resolution World Ocean numerical experiments on simulation of the mechanism of the deep water formation in high latitudes of the North Atlantic. We study the sensitivity of the World ocean fields towards horizontal viscosity and the effects of the dependence of the sea water density on pressure.

1. Introduction

The World ocean is one of the most important components of the climate system. It plays the key role in the climate system. The ocean circulation redistributes heat, and the ocean strongly affects the climate variability on time scales from seasons to millennia. Hence, the accurate modeling of the thermohaline circulation is a crucial task for climate studies. Comprehensive general circulation models usually lack the numerical efficiency to routinely perform simulations over many millennia, but provide a relatively detailed spatial resolution of environmental phenomena. Most of the current models are run at coarse resolution, the grid-spacing being an order of magnitude larger than the Rossby radius of deformation. This model belongs to the "intermediate" or "planetary geostrophic" class of models [8, 12, 13, 17]. The planetary geostrophic models are based on the idea that the momentum balance away from the equator is predominantly geostrophic. The planetary geostrophic formalism allows some simplifications of the momentum equations and a longer time step and, consequently, becomes computationally

*Supported by the Russian Foundation for Basic Research under Grant 05-05-64990.

more effective. Zhang et al. [17] demonstrated that at a coarse-resolution, a purely geostrophic model with linear momentum dissipation for a barotropic flow can reproduce results of the primitive equations [Bryan–Cox] for the evolution of tracer fields, but both are based on the same no-slip boundary condition. There are many problems to which the "planetary geostrophic" models have been successfully applied. Costefficient, dynamic ocean models are necessary to perform millennialscale paleo circulation simulations [9, 12], to represent a wide range of tracers and processes in a coherent dynamic setting [8, 11], to study the deep water formation, and heat global conveyers.

In the previous works [14], a series of numerical experiments with a three-dimensional numerical model of the global ocean climate with real topography and different vertical resolution was described. The temperature of the deep ocean at course resolution has appeared higher, than it should be. With an increasing resolution on the vertical coordinate, the temperature of the deep ocean and the average temperature was close to the observed data. Unfortunately, an increase in resolution does not improve a salinity field. In [15], it was shown that the features of realistic water masses depend on the convection in the polar and subpolar regions, where these water masses are formed. In these regions, the largest density can form only under sufficiently cold and saline values of the water surface data. In [15], such surface temperature and salinity data are manually adjusted to obtain the largest density.

In this paper, we present a three-dimensional model of the World ocean general circulation with 5-degree space resolution along the latitude and the meridian, and 24 levels in the vertical coordinate. This work is a sequel to the results early obtained in [14, 15]. The development of the model is as follows:

- The momentum equations include the Laplacian viscosity and no-slip boundary conditions, while in the previous calculations, we used a horizontal linear friction with no-normal-flow boundary conditions.
- We change the form of the equation of the sea water state, which includes the dependence of water density on pressure. It is based on the UNESCO equation of state for seawater, obtained in the form of a polynomial, [2].

The model satisfactorily reproduces the main structure of currents, temperature and salinity fields.

2. The Model and experimental details

Let us consider the problem of formation of the large-scale climatic temperature, salinity and currents fields in the World ocean including the Arctic ocean with real geometry and bottom topography. It is assumed that the

spatial resolution of the model is large as compared to the internal Rossby radius of deformation ($\gg 50$ km), so nonlinear terms in the Navier–Stokes equations can be neglected, [8].

Consider the initial system of equations, where the hydrostatic, Boussinesq's and rigid lid approximations are employed, and nonlinear terms in the equations of motion are omitted.

The momentum equations are

$$\ell v = -\frac{1}{a\rho_0 \sin\theta}\frac{\partial P}{\partial \lambda} + \frac{\partial}{\partial z}\nu\frac{\partial u}{\partial z} + \frac{A_\ell}{a^2}\Delta u, \tag{1}$$

$$-\ell u = -\frac{1}{a\rho_0}\frac{\partial P}{\partial \theta} + \frac{\partial}{\partial z}\nu\frac{\partial v}{\partial z} + \frac{A_\ell}{a^2}\Delta v; \tag{2}$$

The equation of continuity yields

$$\frac{1}{a\sin\theta}\left(\frac{\partial u}{\partial \lambda} + \frac{\partial v \sin\theta}{\partial \theta}\right) + \frac{\partial w}{\partial z} = 0; \tag{3}$$

The hydrostatic equation is

$$P = -g\rho_0\zeta + g\int_0^z \rho\, dz; \tag{4}$$

The equations of transport of temperature and salinity are

$$\frac{\partial \Phi}{\partial t} + \frac{u}{a\sin\theta}\frac{\partial \Phi}{\partial \lambda} + \frac{v}{a}\frac{\partial \Phi}{\partial \theta} + w\frac{\partial \Phi}{\partial z} = \frac{\partial}{\partial z}\varkappa\frac{\partial \Phi}{\partial z} + \frac{\mu}{a^2}\Delta\Phi, \tag{5}$$

where $\Phi = (T, S)$.

The equation of state is given using the UNESCO-formula

$$\rho = (p, T, S). \tag{6}$$

The boundary conditions for $z = 0$:

$$\begin{aligned} &\nu\frac{\partial u}{\partial z} = -\frac{\tau_\lambda}{\rho_0}, \quad \nu\frac{\partial v}{\partial z} = -\frac{\tau_\theta}{\rho_0}, \quad w = 0, \\ &T = T^*(t, \lambda, \theta), \quad S = S^*(t, \lambda, \theta); \end{aligned} \tag{7}$$

for $z = H$:

$$\begin{aligned} &\nu\frac{\partial u}{\partial z} = -R_2\int_0^H u\, dz, \quad \nu\frac{\partial v}{\partial z} = -R_2\int_0^H v\, dz, \\ &w(H) = \frac{u(H)}{a\cdot\sin\theta}\frac{\partial H}{\partial \lambda} + v(H)\frac{\partial H}{\partial \theta}, \quad \varkappa\frac{\partial T}{\partial z} = 0, \quad \varkappa\frac{\partial S}{\partial z} = 0; \end{aligned} \tag{8}$$

at the lateral wall Γ:

$$\mu\frac{\partial T}{\partial n} = 0, \quad \mu\frac{\partial S}{\partial n} = 0, \quad u = v = 0; \tag{9}$$

at the initial moment $t = 0$:

$$T = \tilde{T}(z), \quad S = \tilde{S}(z). \tag{10}$$

The equations are presented in the spherical coordinate system (λ is latitude, θ is an addition of longitude up to 90°, the axis z is directed vertically downwards); u, v, w are velocity vector components, t is time, ρ_0, ρ are the mean value and the anomaly of density, respectively, $\zeta = \xi - \dfrac{P}{g\rho_0}$ is a reduced level, P is the atmospheric pressure, $z = \xi(\lambda, \theta)$ is the equation of the ocean surface, A_ℓ is the horizontal turbulent viscosity, ν is the vertical turbulent viscosity coefficient, $\varkappa$, μ are the vertical and the horizontal turbulent temperature and salinity diffusion coefficients, $\ell = 2\omega\cos\theta$ is the Coriolis parameter, a, ω, g are the radius, the angular velocity and acceleration of gravity of the Earth, respectively, τ_λ, τ_θ is the wind stress, T^*, S^* are known climatic distributions of temperature and salinity at the surface of ocean, R_2 is the coefficient of the bottom friction, n is the normal to the lateral cylindrical wall Γ, $H(\lambda, \theta)$ is the depth of the ocean,

$$\Delta = \frac{1}{\sin^2\theta}\frac{\partial^2}{\partial\lambda^2} + \frac{1}{sin\theta}\frac{\partial}{\partial\theta}\sin\theta\frac{\partial}{\partial\theta}.$$

The equations are divided into a barotropic and a baroclinic parts by vertical averaging. For this purpose, by representing the horizontal velocity components as $u = \hat{u} + u'$, $v = \hat{v} + v'$, where u', v' is a baroclinic component, $\hat{u}$, $\hat{v}$ is a barotropic component.

Since the vertical averaged flows are nondivergent,

$$\frac{\partial\hat{u}}{\partial\lambda} + \frac{\partial\hat{v}\sin\theta}{\partial\theta} = 0, \quad \hat{u} = \int_0^H u\,dz, \quad \hat{v} = \int_0^H v\,dz.$$

A stream function is defined as

$$\hat{u} = \frac{\partial\psi}{\partial\theta}, \quad \hat{v}\sin\theta = -\frac{\partial\psi}{\partial\lambda}.$$

The stream function equation can be defined as

$$R\Delta_H\psi + \left(\frac{l}{H}, \psi\right) - \frac{\partial}{\partial\lambda}\left(\frac{1}{H}\widetilde{\Delta}m\frac{\partial\psi}{\partial\lambda}\right) - \frac{\partial}{\partial\theta}\left(\frac{n}{H}\widetilde{\Delta}\frac{\partial\psi}{\partial\theta}\right) + m^2\frac{\partial}{\partial\lambda}D\frac{\partial\psi}{\partial\lambda} +$$
$$\frac{\partial}{\partial\theta}D\frac{\partial\psi}{\partial\theta} = \frac{\partial}{\partial\theta}\left\{-\frac{u(H)n}{H}\widetilde{\Delta}H - \frac{2B}{H}\left(m^2\frac{\partial u(H)}{\partial\lambda}\frac{\partial H}{\partial\lambda} + \frac{\partial u(H)}{\partial\theta}\frac{\partial H}{\partial\theta}\right)\right\} -$$
$$\frac{\partial}{\partial\lambda}\left\{-\frac{v(H)}{H}\widetilde{\Delta}H - \frac{2Bm}{H}\left(m^2\frac{\partial v(H)}{\partial\lambda}\frac{\partial H}{\partial\lambda} + \frac{\partial v(H)}{\partial\theta}\frac{\partial H}{\partial\theta}\right)\right\} +$$
$$\frac{g}{a\rho_0}\int_0^H\left(\rho, \frac{z}{H}\right)dz + \mathrm{rot}\,\frac{\vec{\tau}}{H\rho_0},$$

$$\widetilde{\Delta}u = m^2\left(m\frac{\partial}{\partial\lambda}B\frac{\partial u}{\partial\lambda} + n\frac{\partial}{\partial\theta}B\frac{\partial u}{\partial\theta}\right), \quad B = A_\ell n, \quad n = \sin\theta, \quad m = n^{-1},$$

$$\frac{\partial}{\partial\theta}\frac{n}{H}\frac{\partial\psi}{\partial\theta} + \frac{1}{n}\frac{\partial}{\partial\lambda}\frac{1}{H}\frac{\partial\psi}{\partial\lambda} = \Delta_H\psi, \quad \frac{\partial}{\partial\theta}\frac{\tau_\lambda n}{H} - \frac{\partial}{\partial\lambda}\frac{\tau_\theta}{H} = \operatorname{rot}\frac{\vec{\tau}}{H},$$

$$D = \frac{BR_2}{\nu H}\left\{\left(m\frac{\partial H}{\partial\lambda}\right)^2 + \left(\frac{\partial H}{\partial\theta}\right)^2\right\}.$$

The method of solving problem (1)–(10) is described in detail in [16]. Here we only mention that for equation (5) on the uniform five-degree grid the horizontal operator is approximated by the nine-dot difference scheme, obtained by the Richardson extrapolation, and the vertical operator, after introduction of a new variable, condensing the grid at the ocean surface, is approximated by the second up-wind scheme.

The uniform five-degree grid shifted by 2.5° relatively the equator and the lateral boundary Γ is inserted in the polygonal area approximating the World ocean from $72,5°S$ to $87,5°N$. The model includes a realistic smoothed bottom topography. Two grids condescending at the surface of the ocean under the square law are included in the vertical coordinate. On one grid with integer values of the index k

$$z_k = (\eta_N - \eta_0)^2\,[(k-1/2)/N]^2, \tag{11}$$

where $\eta_N^2 = H + \alpha$, $\alpha = 120$ cm, the variables u, v, T, S, ρ are defined. The dots of the second grid lay in the middle of intervals

$$\frac{z_{k+1} + z_k}{2}, \quad z_{1/2} = 0, \quad z_{N+1/2} = H, \tag{12}$$

where $N = 24$ is the number of vertical levels.

In all the experiments, the horizontal diffusion coefficients $\mu_\lambda = \mu_\theta$ were increased by 10^3 on the equator belt of 3 grid step wide. The value of the coefficient A_ℓ near the equator was multiplied by 10^3. Other parameters used in the numerical experiments were:

$$A_\ell = 10^7\text{–}10^8, \quad R_2 = 0.5\cdot 10^{-7}, \quad \nu = 75,$$
$$a = 6.4\cdot 10^8, \quad \omega = 0.73\cdot 10^{-4}, \quad \rho_0 = 1.02541, \quad g = 980.$$

In the experiments, the coefficients of the vertical and the horizontal diffusion $\varkappa$, μ were functions of depth according to [3]. In all the experiments, the global ocean model was forced by the seasonally varying climatic temperature, salinity and wind stress at the ocean surface. The nonlinear advection of momentum has been excluded, the equations being integrated with an implicit method which permits a time step of 10 days.

In all the experiments on the ocean surface, the climatological data on temperature for winter of the northern hemisphere were corrected. The corrections were made for a north-east part of the Northern Atlantic. If in the previous experiments at a grid point the mean value from a five-degree trapezoid was set, the value with a minimum temperature was now selected. In addition, salinity values were corrected for larger values in the places indicated in [1]. These places are close to Greenland and, also, to the Ross and the Weddell seas near Antarctica.

3. The numerical experiments

The numerical experiments Run1, Run2, Run3, and Run4 were to reproduce the climatic structure of temperature, salinity, density and currents fields in the ocean (the table). In each experiment, the model was run until equilibrium. For the first experiments Run1 and Run2, we used the equation of state, without dependence of density on pressure, Unesco-73 [6]. Since the state in question was obtained in the previous experiment, [15], the pattern was integrated for 5000 years more before being stable. In Run1, the mean temperature of the ocean became equal to 4.14 grades, the mean salinity being 34.58 psu. The distribution of the zonally averaged temperature and salinity fields on a meridional plane has unessentially changed. Figures 1, 2 show the profiles of the globally averaged temperature and salinity for all the experiments for the winter season, together with the winter values from Levitus data, [7]. A marked salinity minimum at about 800–1000 m depth is completely absent, the deep water being too fresh.

Summary of the model numerical runs and the results obtained

Exp.	A_ℓ, cm/s^2	State equation	Mean temperature	Mean salinity	ACC, Sv	Heat transport, petawatts	
						noth	south
Run1	10^8	$\rho = (T, S)$, [6]	4.14	34.58	91	0.7	1.4
Run2	10^7	$\rho = (T, S)$, [6]	4.26	34.59	127	0.6	1.3
Run3	10^7	$\rho = (p, T, S)$, [1]	4.10	34.62	176	0.4	1.6
Run4	10^7	$\rho = (p, T, S)$, [1]	4.02	34.66	168	0.6	1.7

Figure 3 shows the meridional volume transport stream function for the global ocean. The general features of the overturning are similar to those obtained in other global models with a similar resolution, [1, 3]. The well-known overturning cells can be identified: a northern sinking cell with a transport of 14 Sv near 60°N, due, primarily, to the North Atlantic Deep Water (NADW) formation; the relatively shallow wind-induced Ekman cell; a southern sinking cell near 35°S; the Deacon cell at latitudes from 35°S to 60°S and an Antarctic circumpolar convective cell.

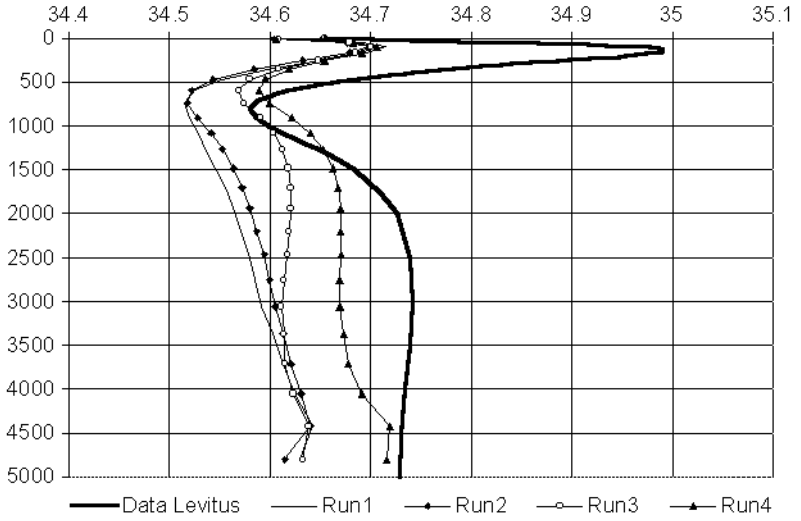

Figure 1. The vertical salinity profiles averaged over the whole World ocean in numerical experiments Run1, Run2, Run3, Run4 and from the Levitus climatological data

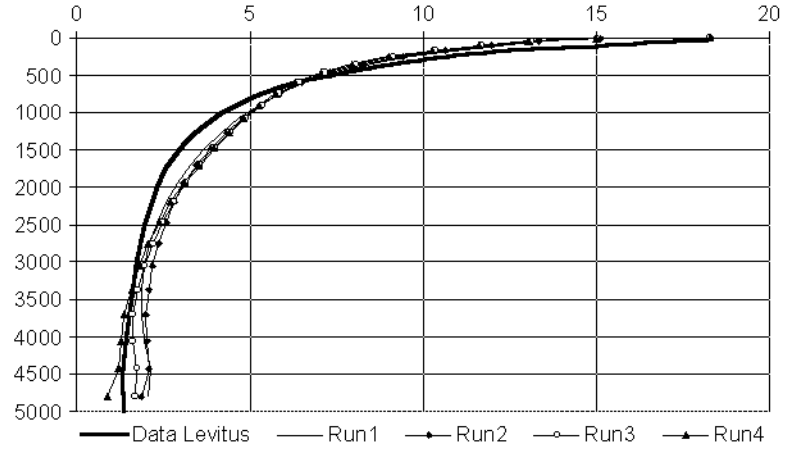

Figure 2. The vertical temperature profiles averaged over the whole World ocean in numerical experiments Run1, Run2, Run3, Run4 and from the Levitus climatological data

In [4], the authors found that the Atlantic water inflow is weak in the case of the viscosity coefficients 10^8 cm^2/s, and this flow significantly increases when viscosity coefficients are scaled down to 10^7 cm^2/s. In experiment Run2, we test the sensitivity of the model to changes in the viscosity coefficient A_ℓ. In model experiment Run2, we use $A_\ell = 1 \cdot 10^7 cm^2/s$. The effect of decreasing the horizontal viscosity is clearly apparent in the simulation of a more real water mass. As well as in the previous experiment, a

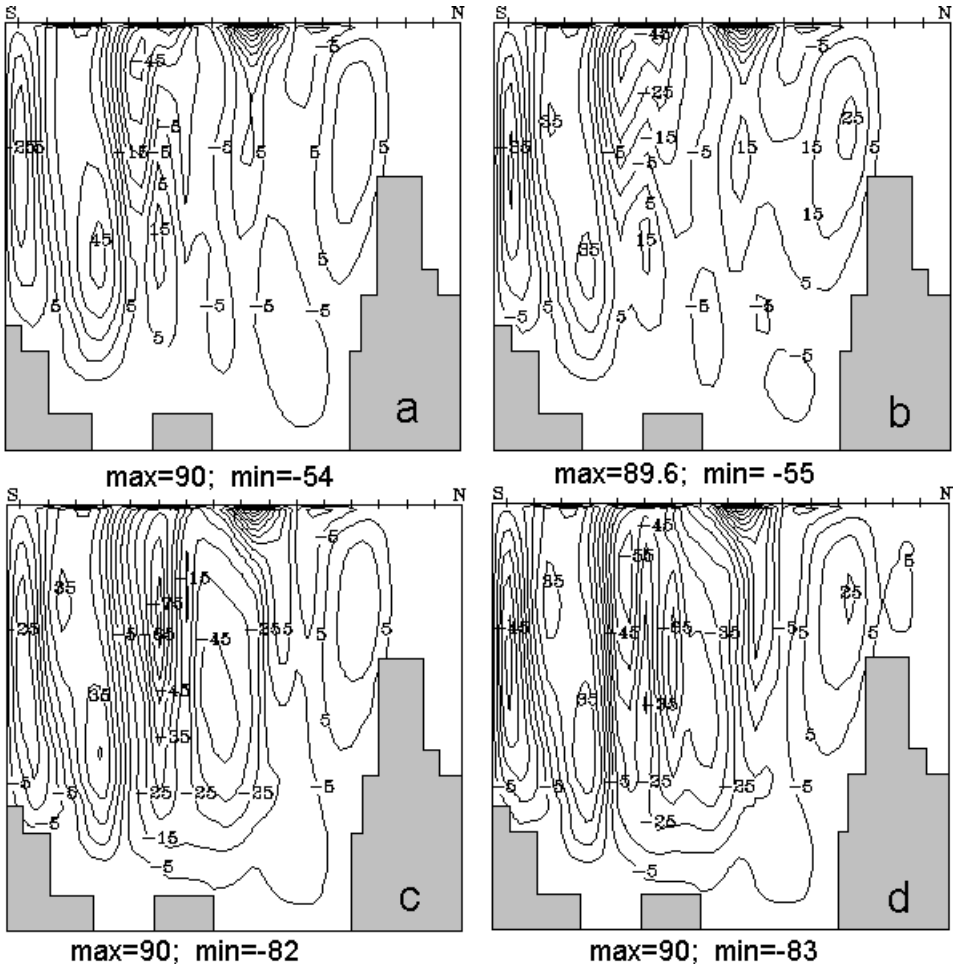

Figure 3. The global zonally-integrated meridional overturning circulation (in sverdrups) for Run1 (a), Run2 (b), Run3 (c), and Run4 (d)

field of heat has practically not varied, though the mean temperature was augmented up to 4.26 grades. The intermediate Antarctic tongue of gentle salt waters has appeared at depth below 500 m, penetrating into the equator, Figure 1b. The low saline Antarctic intermediate waters become more distinct. In Run2, the NADW formation intensifies from 14 (Run1) to 27 Sv (Figure 3a,b). The salt transport increases with the overturning, Figure 4b, thus leading to an even stronger overturning. During this process, the poleward heat transport also increases.

In a flat-bottomed homogeneous ocean, the Antarctic Circumpolar Current (ACC) is in balance between the wind stress and the lateral friction and is very sensitive to changes in the horizontal viscosity, [1]. In an ocean with

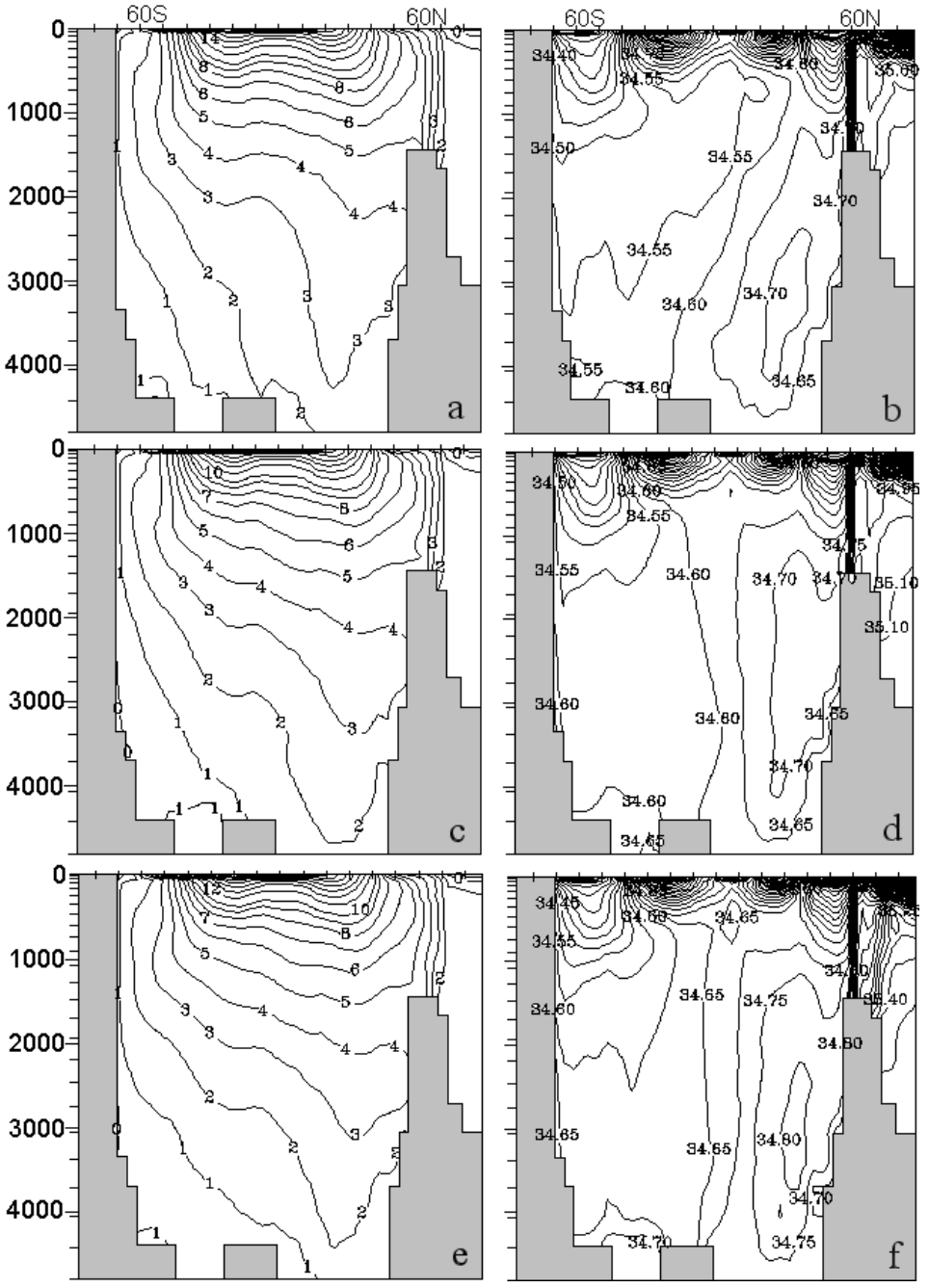

Figure 4. Zonally averaged temperature (a, c, e) and salinity (b, d, f) of the global ocean in the numerical experiments: a, b — Run2, c, d — Run3, e, f — Run4

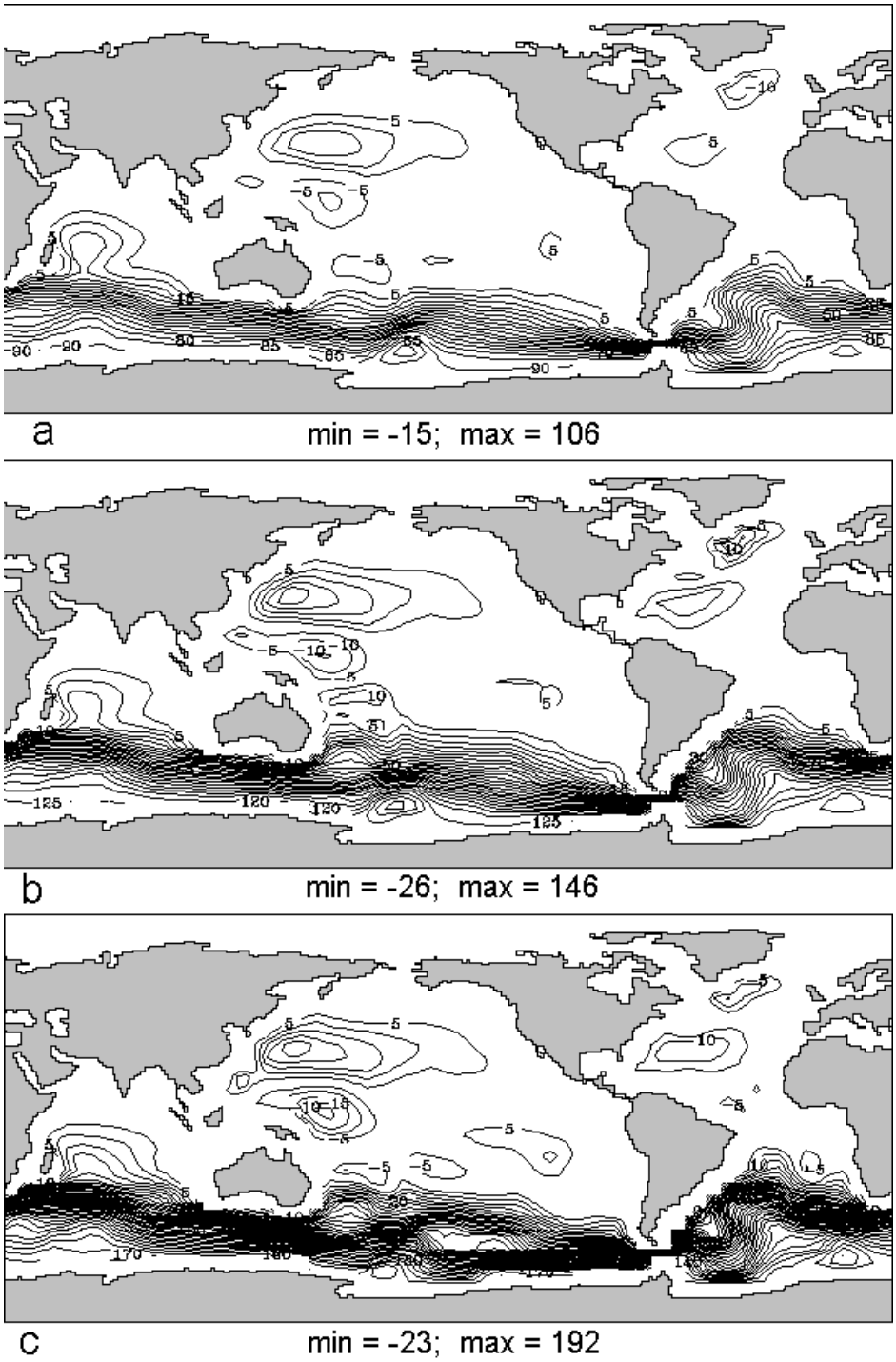

Figure 5. Horizontal barotropic transport stream function (in sverdrups) for Run1 (a), Run2 (b) and Run3 (c)

topography, the ACC is less sensitive to A_ℓ because of the constraints of topography on the current and it increases from 91 to 127 Sv as A_ℓ decreases from 10^8 cm^2/s (Run1) to 10^7 cm^2/s (Run2), Figure 5.

In the next experiment, Run3, we change the form of the equation of the sea water state. The equation is based on the Unesco-80 formula and includes the dependence of water density on pressure, written in the polynomial form [2]. Large modifications have taken place with salinity. The halocline structure of the numerical solution tends to observed profiles (see Figure 1). The vertical profiles of salinity and temperature were qualitatively improved. The mean salinity was increased up to 34.62 psu. Figure 4c shows that the mean temperature of the ocean substantially decreases and becomes equal to 4.1 grades. Thus, the new equation of the sea water state with dependence on pressure is the main factor that allowed to obtain the model temperature and salinity closely approximating to the real one in deep oceanic layers.

The most characteristic difference in the oceanic field when passing to the new equation of state is an increase of the ACC mass transport from 127 to 176 Sv. A similar result was obtained in [10], where the Zalesny model was used. In Run3, the southern sinking cell near 35°S intensifies from 54 (Run2) to 82 Sv, on the contrary, the Atlantic overturning circulation is moderately weakened (see Figure 3c).

In the next experiment, Run4, we change parametrization of the process of convective mixing. At each time step, we calculate a difference in density between the two adjacent levels along the vertical coordinate.

The convection procedure have takes place if

$$\rho(p_{k+1}, T_{k+1}, S_{k+1}) < \rho(p_k, T_k, S_k).$$

Then the temperature and the salinity of these layers will look like:

$$T_{k+1}^{\text{new}} = \frac{T_k + T_{k+1}}{2}, \quad S_{k+1}^{\text{new}} = \frac{S_k + S_{k+1}}{2}.$$

The use of the equation of state, in which the pressure is considered and the use of the above procedure of convective adjustment ensure the conditions of a more intense North Atlantic circulation (see Figure 3d) and the less warm and salter ocean (see Figures 1, 2, 4e, 4f).

4. Conclusions

We have developed the efficient numerical linear model of thermohaline circulation in the World ocean. The model, as a whole, satisfactorily reproduces the main structure of currents, temperature and salinity fields. There is an intrusion of the Antarctic Intermediate Water northwards, which penetrates at depths of 500–1500 m up to the equator and the north tropic

latitude and corresponds well to the observations (see Figure 4b). A similar result was obtained in [1, 3, 5], where the Bryan model was used.

References

[1] Cai W. Interactions between thermohaline- and wind-driven circulations and their relevance to the dynamics of the Antarctic Circumpolar Current, in a coarse-resolution global ocean general circulation model // J. Geoph. Res. — 1996. — Vol. 101, No. C6. — P. 14073–14093.

[2] Brydon D., Sun S., Bleck R. A new approximation of the equation of state for seawater, suitable for numerical ocean models // J. Geoph. Res. — 1999. — Vol. 104, No. C1. — P. 1537–1540.

[3] England M.H. Representing the global-scale water masses in ocean general circulation models // J. Phys. Oceanogr. — 1993. — Vol. 23. — P. 1523–1552.

[4] Golubeva E.N., Platov G.A. On improving the simulation of Atlantic Water circulation in the Arctic Ocean //J. Geoph. Res. — 2007. — Vol. 112, No. C04S05.

[5] Hirst A.C., Cai W. Sensitivity of a World ocean GCM to changes in subsurface mixing parameterization // J. Phys. Oceanogr. — 1994. — Vol. 24. — P. 1256–1279.

[6] International Oceanographic Tables / UNESCO. — 1973. — Vol. 2.

[7] Levitus S. Climatological Atlas of the World Ocean. — U.S. Govt. Printing Office, 1982. — (NOAA Prof. Paper; 13).

[8] Maier-Reimer E., Mikolajewicz U., Hasselmann K. Mean circulation of the Hamburg LSG OGCM and its sensitivity to the thermohaline surface forcing // J. Phys. Oceanogr. — 1993. — Vol. 23. — P. 731–757.

[9] Marchal O., Stocker T.F., Joos F., et al. Modelling the concentration of atmospheric CO2 during the younger dryas climate event // Climate Dynamics. — 1999. — Vol. 15. — P. 341–354.

[10] Moshonkin S.N., Zalesny V.B. Circulation of the World ocean: the effect of physical factors on the formation and the long-term variability of hydrophysical fields // Russ. J. Numer. Anal. Math. Modelling. — 1998. — Vol. 13, No. 6. — P. 517–536.

[11] Plattner G.-K., Joos F., Stocker T.F., et al. Feedback Mechanisms and Sensitivities of Ocean Carbon Uptake under Global Warming. — 2001. — (Tellus; 53).

[12] Seidov D., Haupt B.J. Simulated ocean circulation and sediment transport in the North Atlantic during the last glacial maximum and today Simulated ocean circulation and sediment transport in the North Atlantic during the last glacial maximum and today // Paleoceanography. — 1997. — Vol. 12, No. 2. — P. 281–305.

[13] Seidov D. An intermediate model for large-scale ocean circulation studies // Dyn. Atmos. Oceans. — 1996. — Vol. 25, No. 1. — P. 25–55.

[14] Scherbakov A.V., Malakhova V.V. On sensitivity of the World Ocean model to the vertical resolution // Bull. Novosibirsk Comp. Center. Ser. Num. Model. Atmosph., Ocean and Env. Studies. — Novosibirsk, 1999. — Iss. 4. — P. 53–72.

[15] Scherbakov A.V., Malakhova V.V. On the deep water formation in the World Ocean model // Bull. Novosibirsk Comp. Center. Ser. Num. Model. Atmosph. Ocean and Env. Studies. — Novosibirsk, 2000. — Iss. 6. — P. 73–78.

[16] Scherbakov A.V., Malakhova V.V., Antsis E.N. Numerical model of the World ocean with the Arctic ocean taken into account. — Novosibirsk, 1997. — (Preprint / Computing Center USSR: 1106) (In Russian).

[17] Zhang S., Lin C., Greatbatch R.J. A thermocline model for ocean-climate studies // J. Mar. Res. — 1992. — Vol. 50. — P. 99–124.